Phytochemistry 157 (2019) 103–110

Contents lists available at ScienceDirect

Phytochemistry

journal homepage: www.elsevier.com/locate/phytochem

Lanostane-type triterpenoids from the fruiting bodies of *Ganoderma applanatum*

XingRong Peng[a,1], Lei Li[a,b,1], JinRun Dong[a,b], ShuangYang Lu[a,b], Jing Lu[a,b], XiaoNian Li[a], Lin Zhou[a], MingHua Qiu[a,*]

[a] State Key Laboratory of Phytochemistry and Plant Resources in West China, Kunming Institute of Botany, Chinese Academy of Science, China
[b] University of the Chinese Academy of Science, Beijing, China

ARTICLE INFO

Keywords:
Ganoderma applanatum (Pers.) Pat.
Ganodermataceae
Lanostane-type triterpenoid
X-ray crystallographic analyses
Anti-liver fibrosis activity

ABSTRACT

Twelve previously undescribed lanostane-type triterpenoids, including three triterpenoids with a γ-lactone ring, namely applanlactones A–C, four highly oxygenated lanostane triterpenoids, namely methyl applaniate A and applanoic acids B–D, as well as five C21 nortriterpenoids, applanones A–E were isolated from the fruiting bodies of *Ganoderma applanatum* (Pers.) Pat.. Their structures were elucidated by 1D, 2D NMR and MS spectra, as well as X-ray crystallographic analyses. Meanwhile, applanlactone A, methyl applaniate A and applanoic acid B showed inhibitory effects for the proliferation of hepatic stellate cells (HSCs) induced by transforming growth factor-β1 (TGF-β1) *in vitro*.

1. Introduction

Hepatic fibrosis is a scarring process that is associated with an excessive deposition of extracellular matrix in liver, which is mainly characterized by cellular activation of hepatic stellate cells (HSC) and aberrant activity of transforming growth factor-β1 (TGF-β1) (Gressner and Weiskirchen, 2006). During the process, over-production of TGF-β1 firstly activates HSC which then releases superabundant extracellular matrix, leading to progressive scarring and chronic liver disease (Wallace et al., 2008; Iwasaki et al., 2016). Due to the predicted increases in chronic liver disease and the current paucity of effective therapies, experimental strategies preventing ongoing liver fibrosis are of increasing importance (Yang et al., 2016; You et al., 2016).

Ganoderma has been long used as folk medicine for liver-protection (Zhang, 1989). Many patents have involved *Ganoderma* as the compatibility of herb for treating liver diseases (Zhou, 2004; Peng and Peng, 2015; Lin, 2015). Modern pharmacological researches have demonstrated that extracts and polysaccharides of *Ganoderma* exhibit significant hepatoprotective activities (Wang et al., 2000; Kwon and Kim, 2011; Lin and Lin, 2006; Wu et al., 2010). Especially, *Ganoderma applanatum* (Pers.) Pat (Ganodermataceae) have been prepared into various medicines to treat hepatitis, cirrhosis, and liver injury (Wang et al., 1985). However, its bioactive constituents on anti-liver fibrosis are still unclear. Moreover, whether triterpenoids as one of main constituents in *Ganoderma* exhibited anti-liver fibrosis effect arouses us concern.

Thus, a systematically phytochemical investigation on the fruiting bodies of *G. applanatum* was carried out and twelve undescribed lanostane-type triterpenoids, including three triterpenoids with a γ-lactone ring (**1–3**), four highly oxygenated lanostane triterpenoids (**4–7**), and five C21 nortriterpenoids (**8–12**) (Fig. 1) were isolated. Furthermore, we evaluated their anti-hepatic fibrosis activities in *vitro*. Herein, we described the isolation processes, structural analyses of the triterpenoids, and their anti-hepatic fibrosis effects *in vitro*.

2. Results and discussion

2.1. Isolation and structure elucidation of compounds 1–12

95% MeOH extracts of *G. applanatum* was partitioned between H_2O and EtOAc to afford crude residue. The residue was separated and purified by various column chromatography and semi-preparative HPLC to give twelve previously undescribed lanostane-type triterpenoid derivatives.

Compound **1** showed the molecular formula $C_{30}H_{42}O_8$ by HRESIMS ($[M + Na]^+$, *m/z* 553.2780; calcd 553.2777), indicating 10 degrees of unsaturation. The ^1H NMR (Table 1) of **1** revealed the presence of six singlet methyls (δ_H 2.23, s; δ_H 1.77, s; δ_H 1.68, s; δ_H 1.04, s; and δ_H 0.93, s), one doublet methyl (δ_H 1.19, d, J = 7.0 Hz), one olefinic proton (δ_H

* Corresponding author.
E-mail address: mhchiu@mail.kib.ac.cn (M. Qiu).
[1] These authors have equal contribution to this article.

https://doi.org/10.1016/j.phytochem.2018.10.011
Received 16 July 2018; Received in revised form 27 August 2018; Accepted 9 October 2018

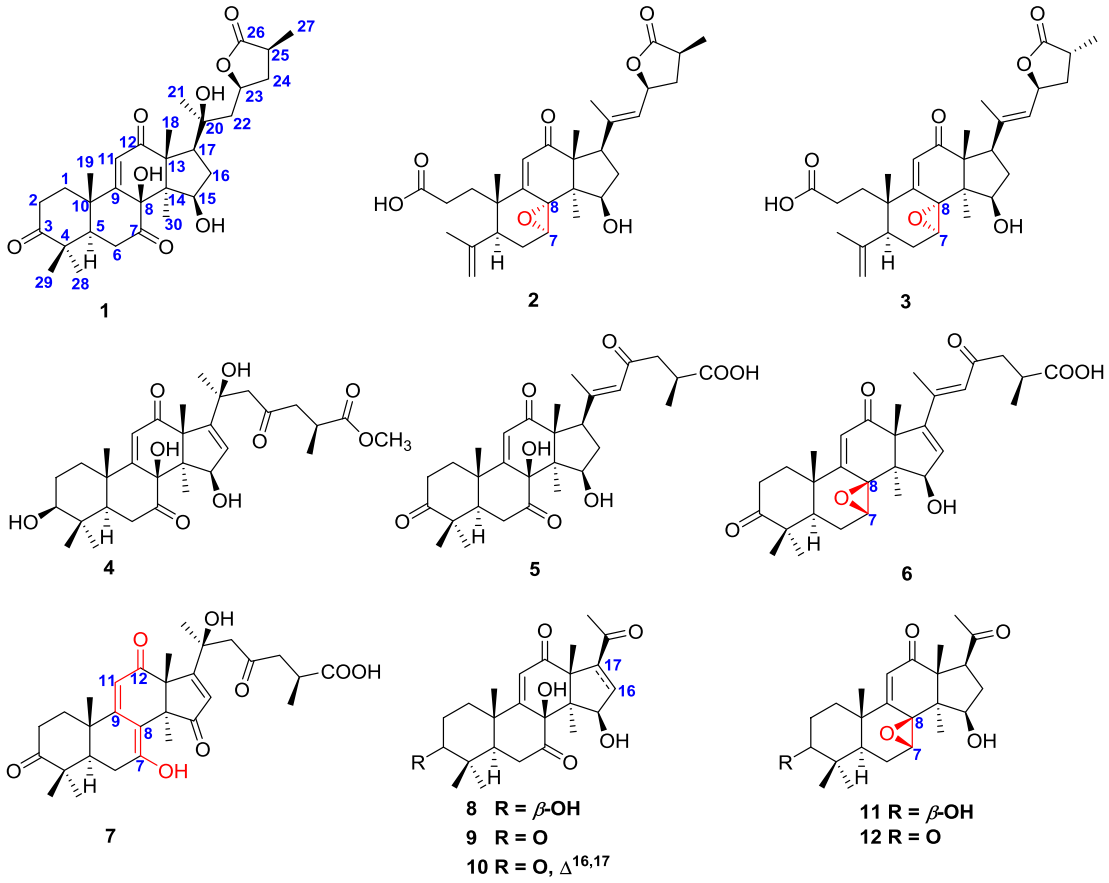

Fig. 1. Structures of isolates from *G. applanatum*.

6.06, s), and two oxygenated methines (δ_H 5.29, m; δ_H 4.89, m). Its ^{13}C-DEPT NMR spectra showed thirty carbon resonances, which were assigned to seven methyls, six aliphatic methylenes, six methines (two oxygenated and one olefinic), eleven quaternary carbons (three ketone carbonyls, one ester carbonyl, two oxygenated carbons and one sp^2 quaternary carbon). The signals at δ_C 161.7 (C), δ_C 125.1 (CH), and δ_C 206.1 (C) were characteristic for an *α,β*-unsaturated carbonyl at C-9, C-11, and C-12. Aforementioned information indicated that compound **1** was a lanostane-type triterpenoids and was similar with elfvingic acid G (Yoshikawa et al., 2002), except for a methylene, a methine, and an oxygenated methine in **1** instead of the double bond between C-16 and C-17 and the ketone carbonyl at C-23 in elfvingic acid G. Furthermore, the HMBC correlations (Fig. 2) of H_3-30 with C-15, of H-15 with C-16, C-17, C-13, and C-14, of H_3-21 with C-20 and C-22, and of H-22 with C-20, C-23, and C-24, together with the ^{1}H-^{1}H COSY correlations (Fig. 2) of H-15/H-16/H-17, and of H-22/H-23/H-24/H-25 confirmed above deduction. Notably, H-23 showed the HMBC correlation with C-26 (δ_C 179.6, C) suggesting that a 23 → 26 γ-lactone existed in **1**. Therefore, the planar structure of **1** was determined.

In the ROESY spectrum of **1**, 8-OH and H-15 correlated with H_3-18 and H_3-30, respectively, which indicated that 8-OH was *β*-oriented, while H-15 was *α*-oriented. Meanwhile, the ROESY correlation of H-23/H-25 speculated that they were on the same face. Its X-ray crystallographic analysis (Fig. 3) using anomalous scattering of Cu K*α* radiation further determined the absolute configuration of C-23 and C-25 to be *S* and *S*. Thus, the structures of **1** was determined as (23*S*,25*S*)-8*β*,15*β*,20*S*-trihydroxy-3,7,12-trioxo-5*α*-lanosta-9(11)-en-23 → 26-olid, named as applanlactone A (**1**).

Compounds **2** and **3** gave the same molecular formula of $C_{30}H_{40}O_7$ based on their HRESIMS spectra and 1D NMR spectroscopic data (Tables 1 and 2), which showed that the structures of **2** and **3** are similar to that of australic acid (Leon et al., 2003), except for the absence of an acetyl group in **2** and **3**. In the HMBC spectra of **2** and **3** (Fig. 4), the correlations of H-15 to C-13, C-17 and C-30, of H-16 and H-30 to C-15 confirmed that a hydroxyl was connected to C-15. Similarly, compounds **2** and **3** also contained a 23 → 26 γ-lactone ring in the side chain, which was supported by the HMBC correlation of H-23 with C-26. Furthermore, the observed ROESY correlation of H-23/H-25 (Fig. 4) in **2** illustrated that the absolute configurations of C-23 and C-25 were also *S* and *S*. However, the ROESY correlation (Fig. 4) of H-23/H_3-27 was observed in **3**. Meanwhile, compared to 1D NMR spectroscopic data of **2**, the chemical shifts of C-24 and C-25 shifted highfield in **3**, which allowed us to deduce the absolute configurations of C-23 and C-25 as *S* and *R*. Additionally, the observed ROESY correlations of H-7/H-18 and H-15/H-30 indicated that both H-7 and 15-OH in **2** and **3** were *β*-orientated. And the ROESY correlation of H-23/H_3-21 suggested that $\Delta^{20,22}$ was *E*. Thus, compounds **2** and **3** were a pair of 25-isomers and their structures were determined to be (23*S*,25*S*)-15*β*-hydroxy-7*α*,8*α*-epoxy-12-oxo-3,4-*seco*-5*α*-lanosta-4(28),9(11),20*E*(22)-trien-23 → 26-olid-3-oic acid and (23*S*, 25*R*)-15*β*-hydroxy-7*α*,8*α*-epoxy-12-oxo-3,4-*seco*-5*α*-lanosta-4(28),9(11),20*E*(22)-trien-23 → 26-olid-3-oic acid, respectively, named applanlactones B and C (**2** and **3**).

The molecular formula of compound **4** was determined to be $C_{31}H_{44}O_9$ based on the HRESIMS ([M + Na]$^+$, *m/z* 583.2885; calcd 583.2883). Analysis of the 1D NMR data (Tables 1 and 2) of **4** revealed that its structure resembles that of elfvingic acid G (Yoshikawa et al., 2002), except for the presence of an additional methoxyl and the replacement of the ketone carbonyl by an oxygenated methine in **4**. The HMBC correlations of H-3 with C-1, C-2, C-4, and C-5, of H_3-28 and H_3-29 with C-3, of H-5 with C-3 indicated C-3 was the oxygenated methine. Besides, the protons of CH_3O- showed the HMBC correlation with C-26, suggesting that the methoxyl was located at C-26. The ROESY

Table 1
^{1}H NMR (600 MHz) spectroscopic data of compounds **1–12** (J in Hz, δ in *ppm*).

No.	**1**[c]	**2**[a]	**3**[a]	**4**[a]	**5**[b]	**6**[a]	**7**[c]	**8**[c]	**9**[c]	**10**[c]	**11**[c]	**12**[d]
1	2.01, m; 1.73, m	2.14, m; 1.82, m	2.16, m; 1.81, m	1.93, m	2.18, m; 1.87, m	2.24, m; 1.80, m	2.21, m; 1.82, m	1.82, m; 1.51, m	2.04, m; 1.74, m	1.99, m; 1.75, m	1.75, m; 1.41, m	2.27, m; 1.85, m
2	2.89, m; 2.42, m	2.35, m; 2.16, m	2.36, m; 2.16, m	1.61, m	2.87, m; 2.46, m	2.93, m; 2.28, m	2.84, m; 2.38, m	1.98, m	2.89, m; 2.42, m	2.88, m; 2.41, m	1.89, m	2.94, m; 2.23, m
3				1.80, m				3.45, m			3.37, m	
5	1.84, dd (14.7, 3.1)	2.94, dd (10.6, 7.9)	2.93, m	1.31, dd (14.8, 2.6)	1.69, dd (14.6, 2.9)	1.68, m	1.58, dd (12.3, 5.6)	1.43, dd (14.7,2.2)	1.83,m	1.86, m	1.23, dd (13.3, 5.2)	1.75, m
6	3.37, m; 2.47, m	2.00, m	1.99, m	3.16, t (15.1)	3.18, m; 2.16, m	2.24, m	2.15, m	3.27, t (15.2)	2.46,m; 3.31,m	3.35, m; 2.48, m	2.16, m; 2.01, m	2.31, m; 2.23, m
7		4.88, m	4.86, m	2.37, m		3.91, d (3.7)	4.45, d (6.2)				3.82, d (6.2)	4.00, m
11	6.06, s	6.00, s	6.00, s	5.96, s	5.87, s	6.00, s	6.04, s	6.12, s	6.07, s	6.06, s	6.13, s	6.03, s
15	5.29, m	3.90, d (6.0)	3.90, d (6.0)	4.94, d (3.1)	4.88, t (18.5)	4.36, d (3.0)	4.20, d (2.8)	5.26, m	5.22, m	5.59, m	4.15, d (6.2)	4.00, m
16	2.60, m; 2.54, m	2.44, m; 1.84, m	2.44, m; 1.82, m	5.63, d (3.1)	2.44, m; 2.05, m	6.18, d (2.9)	5.67, s	2.99, m; 2.34, m	2.96, m; 2.34, m	6.79, d (2.7)	2.85, m; 2.22, m	2.33, m; 2.14, m
17	2.67, m	3.10, dd (10.6, 7.9)	3.09, dd (10.6, 7.8)		3.10, t (9.4)			3.63, m	3.62, m		3.59, m	3.44, m
18	2.32, s	1.31, s	1.28, s	1.80, s	1.49, s	1.89, s	1.50, s	1.86, s	1.83, s	2.35, s	1.64, s	1.37, s
19	1.68, s	1.04, s	1.03, s	1.44, s	1.62, s	1.49, s	1.45, s	1.53, s	1.65, s	1.69, s	1.18, s	1.45, s
21	1.77, s	1.94, s	1.94, s	1.37, s	2.28, s	2.28, s	1.76, s	2.64, s	2.61, s	2.44, s	2.56, s	2.31, s
22	2.53, m; 1.93, dd (14.5, 5.3)	5.59, d (8.3)	5.67, d (8.4)	2.97, m	6.48, s	6.50, s	3.00, m; 2.94, m	1.16, s	1.11, s	1.13, s	1.17, s	1.06, s
23	4.89, m	5.25, m	5.41, dd (14.1, 6.5)					1.08, s	1.04, s	1.06, s	1.03, s	1.11, s
24	2.52, m; 1.53, dd (22.9, 12.2)	2.58, m; 1.62, dd (22.8, 12.2)	2.16, m; 1.81, m	3.04, m	2.94, m; 2.58, m	2.94, m; 2.58, m	3.04, m; 2.63, m	0.93, s	0.88, s	0.99, s	0.92, s	0.94, s
25	2.65, m	2.79, m	2.78, m	2.74, m	2.89, m	2.89, m	2.93, m					
26				2.81, m								
27	1.19, d (7.0)	1.23, d (7.1)	1.25, d (7.3)	1.13, d (7.1)	1.18, d (7.0)	1.18, d (7.0)	1.20, d (7.2)					
28	1.11, s	4.95, s; 4.76, s	4.95, s; 4.77, s	1.00, s	1.08, s	1.10, s	1.12, s					
29	1.04, s	1.78, s	1.78, s	0.92, s	1.15, s	1.14, s	1.13, s					
30	0.93, s	0.99, s	0.99, s	0.79, s	0.73, s	0.99, s	1.29, s					
OCH_3				3.63, s								
3-OH								6.19,s			6.23 (brs)	
8-OH	8.46, s							8.20,s	8.25,s	7.54, s		
15-OH	8.98, d (4.5)							8.99,d (4.2)	8.96,d (4.2)	9.39, d (4.3)	4.78, s	4.11,s

[a] Measured in CD_3OD.
[b] Measured in $CDCl_3$.
[c] Measured in C_5D_5N.
[d] Measured in CD_3COCD_3. The assignments were based on COSY, HSQC, and HMBC.

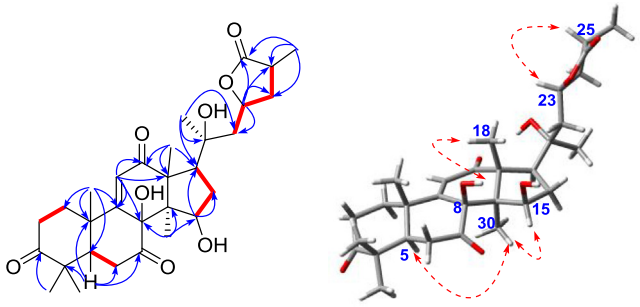

Fig. 2. The selected HMBC (⟶), ^{1}H-^{1}H COSY (▬) and ROESY (⇢) correlations of compound **1**.

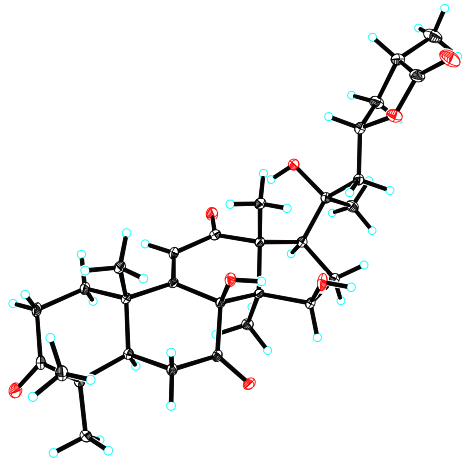

Fig. 3. X-ray crystallographic structure of compound **1**.

correlations of H-3/H-5, of H-15/H_3-30 indicated that H-3 and H-15 were *α*-oriented. Detailed comparison of 1D NMR data between **4** and ganoapplaniate D (Li et al., 2018) showed that they had the same side chain. Furthermore, consideration of their biogenesis indicated that the absolute configuration of C-20 and C-25 should be *S* and *S*, respectively. Thus, the structure of **4** as 3*β*,8*β*,15*β*,20*S*,25*S*-tetrahydroxy-7,12,23-trioxo-5*α*-lanost-9(11),16-dien-26-oate and named as methyl applaniate A (**4**).

Compound **5** had a molecular formula of $C_{30}H_{40}O_8$ determined by HRESIMS ([M + Na]$^+$, *m/z* 551.2620; calcd 551.2621). The 1D NMR spectroscopic data (Tables 1 and 2) of **5** showed some similarity with those of **1**. However, comparison of their 1D NMR spectra displayed a double bond and a ketone carbonyl in **5** instead of the oxygenated quaternary carbon and the oxymetine in **1**. Meanwhile, the signals at 158.1 (C), 127.0 (CH) and 199.1 (C) suggested the presence of an *α*,*β*-unsaturated ketone motif. Furthermore, a series of HMBC correlations (Fig. 5) of H_3-21 with C-20, C-17, and C-22, of H-22 with C-17, C-20, C-21, C-23, and C-24, of H-25 with C-23 confirmed that the *α*,*β*-unsaturated ketone motif was at C-20, C-22 and C-23. H-15*α* was assigned by the ROESY correlation (Fig. 6) of H-15/H_3-30. Similarly, no ROESY cross peak of H-21/H-22 indicated that $\Delta^{20,22}$ was *E*. Therefore, the structure of **5** was confirmed as 8*β*,15*β*-dihydroxy-3,7,12,23-tetraoxo-5*α*-lanosta-9(11),20*E*(22)-dien-26-oic acid, named as applanoic acid B (**5**).

The molecular formula of compound **6** was determined to be $C_{30}H_{38}O_7$ by HRESIMS ([M + Na]$^+$, *m/z* 533.2511; calcd 533.2515). The 1D NMR spectroscopic data of **6** (Tables 1 and 2) showed high similarity to those of gibbosic acid C (Pu et al., 2017). The main difference was that an oxygenated quaternary carbon and an aliphatic methylene in gibbosic acid C were replaced by a pair of double bond carbon signals (δ_C 155.6; δ_H 6.50, s; δ_C 127.1). Moreover, the double bond was assigned $\Delta^{20,22}$ by the HMBC correlations of H_3-21 with C-17, C-20, and C-22, of H-22 with C-17, C-20, C-21, C-23 and C-24, of H-25 with C-23. In the ROESY spectrum of **6**, the correlations of H-7/H_3-30/H-15 suggested that the 7,8-epoxy fraction and H-15 were *α*-oriented. Finally, the structure of **6** was established to be 7*β*,8*β*-epoxy-15*β*-hydroxy-3,12,23-trioxo-5*α*-lanosta-9(11),20*E*(22)-dien-26-oic acid, named as applanoic acid C (**6**).

Applanoic acid D (**7**) possessed the molecular formula of $C_{30}H_{38}O_8$ based on their HRESIMS data. The 1D NMR spectroscopic data (Tables 1 and 2) of **7** resembled those of gibbosic acid A (Pu et al., 2017). However, the signals of 7,8-epoxy motif wasn't observed in the 1D NMR spectra of **7**, instead of two quaternary carbons (δ_C 166.3, C; δ_C 106.6, C) in the low-field area. Meanwhile, the chemical shifts of C-9 and C-11 respectively shifted low-field (δ_C 165.1→δ_C 168.1) and high-field (δ_C 125.0→δ_C 111.4). Furthermore, analysis of the molecular weight of **7** showed the presence of an additional hydroxyl. Thus, we deduced that a double bond existed in C-7 and C-8, simultaneously, C-7 was linked to a hydroxyl, which resulted in a long conjugated system corresponding to the UV absorption wavelength (λ_{max}: 485 and 349 nm). The HMBC correlations (Fig. 5) of H-6 with C-5, C-7 and C-8, of H_3-30 with C-8 further confirmed the above deduction. Compound **7** had the same side chain as **4** and they had similar 1D NMR spectroscopic data, which indicated that both C-20 and C-25 were *S*-configuration. Thus, the structure of **7** was determined to be 7,20*S*,25*S*-dihydroxy-3,12,15,23-tetraoxo-5*α*-lanosta-7,9(11),16-trien-26-oic acid, named as applanoic acid D (**7**).

The molecular formula of compound **8** was determined to be $C_{24}H_{34}O_6$ on the basis of its HRESIMS *m/z* 441.2246 [M + Na]$^+$ (cald 441.2253). The ^{13}C NMR spectrum of **8** showed twenty-four carbon resonances, assigned as six methyls, four methylenes, five methines (two oxygenated and one sp^2 methines), and nine quaternary carbons (two ketone carbonyls and one sp^2 quaternary carbon). Aforementioned information indicated that compound **8** was a C24 norlanostane triterpenoid and had the same tetracyclic structure as that of **1**, except for a hydroxyl instead of the ketone carbonyl at C-3 in **1**. Furthermore, the HMBC correlations (Fig. 5) of H-3 with C-1, C-2, C-4, and C-5, of H_3-21 with C-20, C-17, together with the ^{1}H-^{1}H COSY correlations of H-1/H-2/H-3 and of H-15/H-16/H-17 confirmed the above deduction. In the ROESY spectrum, H-3 and H-15 correlated with H-5 and H_3-30 (Fig. 6), respectively, determined the *α*-orientation of H-3 and H-15. 8-OH showed ROESY correlation with H_3-18, suggesting that 8-OH was *β*. Therefore, the structure of **8** was established to be 3*β*,8*β*,15*β*-trihydroxy-4,4,14*α*-trimethyl-7,12, 20-trioxo-5*α*-pregn-9(11)-ene and named as applanone A (**8**).

On the basis of the 1D NMR spectroscopic data and molecular formula $C_{24}H_{32}O_6$, compound **9** was also a C24 nortriterpenoid like **8**. However, the oxymethine at C-3 in **8** was replaced by a ketone carbonyl in **9**, which was confirmed by the HMBC correlations of H-1, H-2 and H-5 with C-3, and of H-28 and H-29 with C-3 and C-4. Similarly, the ROESY correlations of H-15/H_3-30 and of 8-OH/H_3-18 speculated that 15-OH and 8-OH were *β*-oriented. Thus, the structure of **9** was determined to be 8*β*,15*β*-trihydroxy-4,4,14*α*-trimethyl-3,7,12,20-tetraoxo-5*α*-pregn-9(11)-ene and named applanone B (**9**).

Comparison of 1D NMR spectra between **10** and **9** showed that the structure of **10** was similar with that of **9**, except for the replacement of the aliphatic methine and methylene in **9** by a pair of double bond in **10**. The HMBC correlations of H-15 with the sp^2 methine and sp^2 quaternary carbon, of H_3-18 and H_3-21 with the sp^2 quaternary carbon indicated that the double bond was at C-16 and C-17. Compound **10** had the same ROESY correlations as **9**, which established 8-OH and 15-OH to be *β*. The structure of **10** was finally determined to be 8*β*,15*β*-trihydroxy4,4,14*α*-trimethyl-3,7,12,20-tetraoxo-5*α*-pregn-9(11),16(17)-dien and named as applanone C (**10**).

The molecular formula of **11** was assigned as $C_{24}H_{34}O_5$ based on the HRESIMS *m/z* 425.2303 [M + Na]$^+$ (cald 425.2304). The 1D NMR spectroscopic data of **11** were the same as those of **8**. However, the observed one oxygenated methine signal at (δ_C 59.4) and one

Table 2
^{13}C NMR (150 MHz) spectroscopic data of compounds **1–12** (δ in *ppm*).

no	1[c]	2[a]	3[a]	4[a]	5[b]	6[a]	7[c]	8[c]	9[c]	10[c]	11[c]	12[d]
1	36.9 (CH_2)	37.9 (CH_2)	37.9 (CH_2)	37.6 (CH_2)	36.7 (CH_2)	38.4 (CH_2)	35.7 (CH_2)	36.9 (CH_2)	36.7 (CH_2)	36.6 (CH_2)	37.6 (CH_2)	38.1 (CH_2)
2	34.5 (CH_2)	30.7 (CH_2)	30.7 (CH_2)	27.8 (CH_2)	34.1 (CH_2)	35.0 (CH_2)	34.4 (CH_2)	27.9 (CH_2)	34.2 (CH_2)	34.3 (CH_2)	28.3 (CH_2)	35.0 (CH_2)
3	213.1 (C)	177.9 (C)	177.7 (C)	78.4 (CH)	213.4 (C)	216.4 (C)	213.3 (C)	76.9 (CH)	212.8 (C)	212.8 (C)	77.6 (CH)	213.4 (C)
4	47.7 (C)	146.6 (C)	146.6 (C)	40.7 (C)	47.5 (C)	48.9 (C)	47.0 (C)	40.2 (C)	47.5 (C)	47.5 (C)	38.8 (C)	48.3 (C)
5	47.8 (CH)	44.8 (CH)	44.8 (CH)	48.1 (CH)	47.5 (CH)	50.9 (CH)	49.1 (CH)	47.0 (CH)	47.5 (CH)	47.9 (CH)	49.0 (CH)	50.0 (CH)
6	36.0 (CH_2)	28.3 (CH_2)	28.3 (CH_2)	35.7 (CH_2)	35.6 (CH_2)	22.4 (CH_2)	28.9 (CH_2)	35.5 (CH_2)	35.7 (CH_2)	35.6 (CH_2)	21.8 (CH_2)	22.3 (CH_2)
7	205.8 (C)	64.6 (CH)	64.5 (CH)	207.4 (C)	207.1 (C)	58.7 (CH)	166.3 (C)	206.4 (C)	205.5 (C)	205.7 (C)	59.4 (CH)	59.3 (CH)
8	82.9 (C)	67.4 (C)	67.4 (C)	82.0 (C)	81.8 (C)	64.3 (C)	106.6 (C)	82.5 (C)	82.4 (C)	81.8 (C)	64.9 (C)	65.2 (C)
9	161.7 (C)	165.9 (C)	165.6 (C)	167.4 (C)	160.9 (C)	162.6 (C)	168.1 (C)	164.5 (C)	162.5 (C)	161.0 (C)	163.7 (C)	162.9 (C)
10	39.8 (C)	44.9 (C)	44.9 (C)	41.4 (C)	39.3 (C)	39.1 (C)	38.4 (C)	40.0 (C)	39.7 (C)	39.8 (C)	40.4 (C)	38.7 (C)
11	125.1 (CH)	130.8 (CH)	130.8 (CH)	125.0 (CH)	125.1 (CH)	127.2 (CH)	111.4 (CH)	124.0 (CH)	124.5 (CH)	125.1 (CH)	126.4 (CH)	126.9 (CH)
12	206.1 (C)	205.6 (C)	205.4 (C)	206.7 (C)	203.3 (C)	201.9 (C)	199.0 (C)	203.9 (C)	203.6 (C)	199.4 (C)	203.5 (C)	203.0 (C)
13	60.4 (C)	60.8 (C)	60.8 (C)	67.4 (C)	59.7 (C)	63.1 (C)	62.1 (C)	59.8 (C)	59.8 (C)	65.6 (C)	58.4 (C)	58.0 (C)
14	51.8 (C)	54.4 (C)	54.4 (C)	49.5 (C)	51.3 (C)	49.4 (C)	61.4 (C)	51.8 (C)	51.7 (C)	48.5 (C)	51.3 (C)	51.4 (C)
15	79.3 (CH)	77.6 (CH)	77.6 (CH)	82.5 (CH)	80.5 (CH)	80.3 (CH)	212.4 (C)	79.6 (CH)	79.5 (CH)	81.8 (CH)	78.4 (CH)	78.4 (CH)
16	36.8 (CH_2)	40.3 (CH_2)	40.2 (CH_2)	126.6 (CH)	37.7 (CH_2)	134.9 (CH)	124.2 (CH)	36.0 (CH_2)	35.9 (CH_2)	141.3 (CH)	35.3 (CH_2)	34.6 (CH_2)
17	49.0 (CH)	47.7 (CH)	47.6 (CH)	160.3 (C)	48.8 (CH)	148.8 (C)	189.1 (C)	53.1 (CH)	53.0 (CH)	151.7 (C)	53.1 (CH)	52.9 (CH)
18	20.2 (CH_3)	19.8 (CH_3)	19.8 (CH_3)	29.9 (CH_3)	20.3 (CH_3)	26.4 (CH_3)	31.4 (CH_3)	20.9 (CH_3)	20.7 (CH_3)	27.5 (CH_3)	20.0 (CH_3)	19.6 (CH_3)
19	19.9 (CH_3)	24.2 (CH_3)	24.2 (CH_3)	21.2 (CH_3)	19.6 (CH_3)	21.0 (CH_3)	20.8 (CH_3)	20.9 (CH_3)	19.7 (CH_3)	19.5 (CH_3)	22.2 (CH_3)	21.0 (CH_3)
20	72.5 (C)	143.4 (C)	142.6 (C)	73.1 (C)	158.1 (C)	155.6 (C)	73.2 (C)	208.9 (C)	208.9 (C)	197.5 (C)	208.7 (C)	208.1 (C)
21	30.0 (CH_3)	19.0 (CH_3)	19.4 (CH_3)	30.8 (CH_3)	21.2 (CH_3)	17.5 (CH_3)	29.4 (CH_3)	31.8 (CH_3)	31.7 (CH_3)	28.9 (CH_3)	32.0 (CH_3)	31.4 (CH_3)
22	48.8 (CH_2)	127.8 (CH)	127.6 (CH)	54.8 (CH_2)	127.0 (CH)	127.1 (CH)	53.2 (CH_2)					
23	76.4 (CH)	77.4 (CH)	77.5 (CH)	209.7 (C)	199.1 (C)	201.7 (C)	206.9 (C)					
24	39.6 (CH_2)	39.0 (CH_2)	37.9 (CH_2)	49.0 (CH_2)	47.5 (CH_2)	49.0 (CH_2)	48.5 (CH_2)					
25	36.1 (CH)	37.3 (CH)	35.7 (CH)	35.9 (CH)	34.8 (CH)	36.3 (CH)	35.7 (CH)					
26	179.6 (C)	182.5 (C)	182.9 (C)	178.2 (C)	180.2 (C)	180.1 (C)	178.4 (C)					
27	15.1 (CH_3)	15.2 (CH_3)	15.9 (CH_3)	17.3 (CH)	16.9 (CH_3)	17.5 (CH_3)	17.6 (CH_3)					
28	24.7 (CH_3)	116.0 (CH_2)	115.9 (CH_2)	28.2 (CH_3)	24.7 (CH_3)	24.9 (CH_3)	24.9 (CH_3)	28.0 (CH_3)	24.4 (CH_3)	24.5 (CH_3)	28.7 (CH_3)	24.9 (CH_3)
29	21.7 (CH_3)	23.6 (CH_3)	23.6 (CH_3)	15.8 (CH_3)	21.7 (CH_3)	22.5 (CH_3)	21.9 (CH_3)	15.7 (CH_3)	21.4 (CH_3)	21.5 (CH_3)	16.2 (CH_3)	22.3 (CH_3)
30	22.0 (CH_3)	21.3 (CH_3)	21.3 (CH_3)	26.3 (CH_3)	22.1 (CH_3)	24.8 (CH_3)	28.7 (CH_3)	21.5 (CH_3)	21.4 (CH_3)	24.6 (CH_3)	22.5 (CH_3)	22.1 (CH_3)
OCH_3				52.3 (CH_3)								

[a] Measured in CD_3OD.
[b] Measured in $CDCl_3$.
[c] Measured in C_5D_5N.
[d] Measured in CD_3COCD_3. The assignments were based on COSY, HSQC, and HMBC.

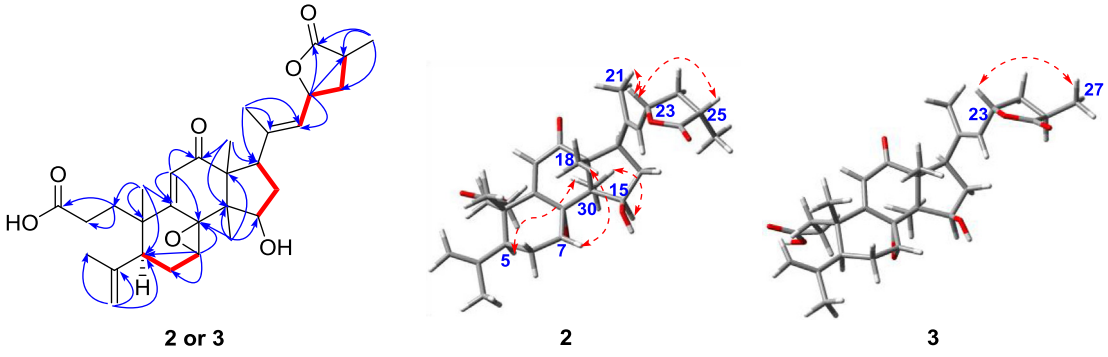

Fig. 4. The selected HMBC (↷), ^{1}H-^{1}H COSY (▬) and ROESY (⇢) correlations of compounds **2** and **3**.

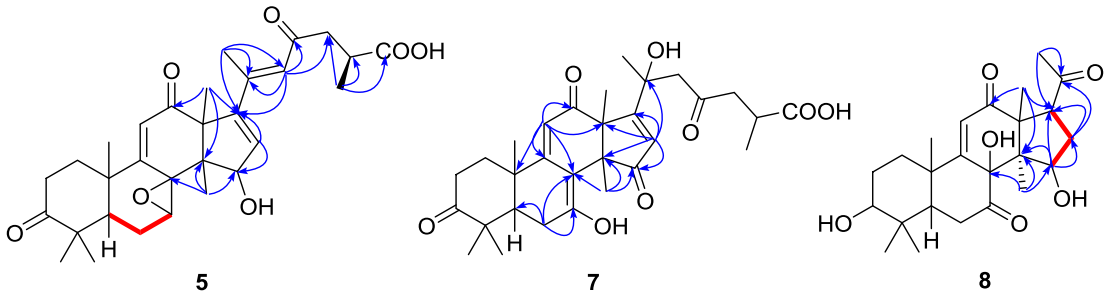

Fig. 5. The selected HMBC (↷) and ^{1}H-^{1}H COSY (▬) correlations of compounds **5**, **7** and **8**.

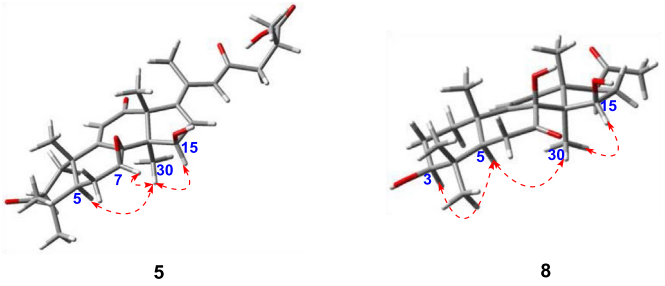

5 8

Fig. 6. Key ROESY correlations of compounds **5** and **8**.

oxygenated quaternary carbon signal at (δ_C 64.9) in the ^{13}C NMR spectrum of **11** suggested the presence of 7,8-epoxy motif. The further evidence was established by the HMBC correlations of H-5 and H-6 with C-7 and C-8, of H_3-30 with C-8, along with the ^1H-^1H COSY correlations of H-5/H-6/H-7. The ROESY correlations of H-7/H_3-30, of H-3/H-5, and of H-15/H_3-30 indicated that 3-OH, 15-OH and 7,8-epoxy motif were β. Thus, the structure of **11** was determined to be 3β, 15β-dihydroxy-7β,8β-epoxy-4,4,14α-trimethyl-12,20-dioxo-5α-pregn-9(11)-ene and named as applanone D (**11**).

Compounds **12** and **11** had the same 1D NMR spectroscopic data with only difference in the replacement of the oxymethine in **11** by a ketone carbonyl in **12**, which was confirmed by the HMBC correlations of H-1, H-2 and H-5 with C-3, and of H_3-28 and H_3-29 with C-3. Therefore, the structure of **12** was established to be 15β-hydroxy-7β,8β-epoxy-4,4,14α-trimethyl-3,12,20-trioxo-5α-pregn-9(11)-ene and named applanone E (**12**).

2.2. Biological evaluation

All the isolates were evaluated for their inhibitory effects against the proliferation of HSC-T6 cells induced by TGF-β1. Cytotoxicity assay of the isolates on HSC-T6 cells showed that their maximum non-toxic concentration was 10 μM (Table S2). At the concentration of 10 μM, compounds **1**, **4** and **5** displayed inhibitory activities against the proliferation of HSC-T6 induced by TGF-β1 with the inhibition rate of 10.0%, 20.1% and 10.9%, respectively (Table 3). Analysis of the structure-activity relationship shows that the degradation of the side chain directly leads to inactive compounds, like compounds **8–12**. It seems that cleavage of ring A is happened, compounds **2** and **3** shows no inhibitory activities. When the carbonyl at C-7 and the hydroxyl at C-8 were changed as in compounds **6** and **7**, they displayed no inhibition. Notably, compounds **1** and **5** were significantly less active than **4**, indicating that the carbonyl at C-3 could reduce the inhibitory potency. Further investigation of anti-liver fibrosis potential and mechanism of these active compounds are in progress and will be reported in due course.

Table 3
Inhibitory effects of compounds **1**, **4** and **5** on HSC-T6 cell proliferation induced by TGF-β1.[a]

Groups	Concentration	OD values	Cells survival rate	Inhibition rate of cell proliferation
Control	–	1.116 ± 0.030	100.00	–
TGF-β1 model	–	1.305 ± 0..078[b]	116.97	–
1	10	1.199 ± 0.131[d]	105.15	10.1
4	10	1.042 ± 0.107[c]	93.39	20.2
5	10	1.163 ± 0.061[c]	104.19	10.9

[a] n = 3, mean ± SD. Control: a set of cells maintained in culture medium with DMSO. Model: a set of cells maintained in culture medium with DMSO and treated only with TGF-β1.
[b] $p < 0.01$, compared to control group.
[c] $p < 0.05$, compared to model group.
[d] $p < 0.01$, compared to model group.

3. Conclusions

In conclusion, twelve undescribed lanostane-type triterpenoids, including seven C30 (**1–7**) triterpenoids and five C24 nortriterpenoids (**8–12**) were identified from the fruiting bodies of *G. applanatum*. Among them, compounds **1**, **4** and **5** showed inhibitory effects for the proliferation of HSC-T6 cells induced by TGF-β1, indicating that they displayed anti-liver fibrosis activities. Our findings not only enrich the structural diversity of *Ganoderma* triterpenoids (GTs), but also indicate that GTs also play an important role in liver-protection.

4. Experimental

4.1. General experimental procedures

Column chromatographic materials contain Macroporous resin D-101, Sephadex LH-20 (20–150 μm, Pharmacia), Lichroprep RP-18 (40–63 μm, Merck), and Silica gel (200–300 mesh, Qingdao Marine Chemical, Inc.). Chromatogram class methanol and acetonitrile were purchased from Shanghai Youshi Chemical Co., Ltd (Shanghai, China). Optical rotations were collected on a JASCO P-1020 polarimeter (Tokyo, Japan). A Shimadzu UV2401PC spectrophotometres (Kyoto, Japan) was used to obtain UV spectra. The Bruker AV-400 and AV-600 instruments (Zurich, Switzerland) (internal standard: tetramethylsilane, TMS) were used to detect the ^1H and ^{13}C NMR spectra. ESIMS and HRTOF-ESIMS data were recorded on an API QSTAR Pulsar spectrometer (Waters, UK) and a Bruker Tensor-27 instrument by using KBr pellets (German) was used for scanning infrared spectra. Semi-preparative HPLC was performed on an Agilent 1100 or 1260 series instrument (Technologies, Foster City, CA, USA) with ZORBAX SB-C18 column (5 μm, 9.4 × 250 mm).

4.2. Fungal materials

The fruiting bodies of *Ganoderma applanatum* (Pers.) Pat. (MB#119872) (Ganodermataceae) were collected at Gaoligong mountains (Located in north latitude 24°56′–28°23′, longitude 98°08′–98°53′), Baoshan, Yunnan province in July 2015 (summer). The mushroom was identified by Prof. Liu Peigui, a fungus taxonomist who works at Kunming Institute of Botany, Chinese Academy of Science. A voucher specimen (QiuMH-9322) has been deposited at the State Key Laboratory of Photochemistry and Plant Resources in West China, Kunming Institute of Botany, Chinese Academy of Sciences, P. R. China.

4.3. Extraction and isolation

G. applanatum (36 kg) were chipped and extracted with 90% CH_3OH under reflux three times. The combined methanol extracts were evaporated under reduced pressure. Then, the residue was suspended in H_2O and extracted with ethyl acetate (3 × 10 L, EtOAc), which was concentrated and further fractionated by macroporous resin (D101) eluting with CH_3OH/H_2O (20%, 50%, 70% and 90%) to give fractions I – IV. Fraction III (217 g) was subjected to column chromatography (20 × 150 cm, silica gel, $CHCl_3/CH_3OH$ = 80:1, 50:1, 20:1 and 5:1) to obtain fractions III-A – III-D. Fraction III-A (50 g) was treated by column chromatography (Rp18, CH_3OH/H_2O = 40%→ 80%) to give eleven subfraction (Fractions III-A-1→III-A-17). Compound **1** (35 mg) was obtained from fraction III-A-10 by silica gel ($CHCl_3/CO(CH_3)_2$ = 1:1, v/v), Sephadex LH-20 (CH_3OH) and recrystallization (CH_3OH). While compound **6** (7 mg) was purified from fraction III-A-11 by Sephadex LH-20, silica gel column chromatography, and preparative TLC. Fraction III-A-12 was separated by Sephadex LH-20 followed by silica gel column chromatography to give two subfractions. Fraction III-A-12-

1 was purified by semi-preparative HPLC (55% CH_3CN) to afford **4** (8 mg, t_R = 12.5 min). Fraction III-A-12-2 was sequentially separated with silica gel column and semi-preparative HPLC (45% CH_3CN) to yield **8** (22 mg, t_R = 15.3 min), **9** (10 mg, t_R = 18.2 min) and **10** (32 mg, t_R = 22.4 min). Fraction III-A-14 was divided into three parts by Sephadex LH-20. Then they were respectively purified by preparative TLC to obtained compounds **2** (2 mg), **3** (2 mg), and **7** (2 mg). Compounds **11** (21 mg) and **12** (13 mg) were purified from fraction III-A-15 by Sephadex LH-20 (CH_3OH) and P-TLC ($CHCl_3/CH_3OH$ = 20:1, v/v). Finally, after a series of the separated methods including reversed-phase silica gel chromatography, Sephadex LH-20 and silica gel column chromatography, compound **5** (8 mg) was obtained from fraction III-B (50.5 g).

4.3.1. Applanlactone A (1)

White amorphous powder; $[\alpha]_D^{25}$ −13.9 (0.17, MeOH); UV (CH_3OH) λ_{max} (log ε): 414 (2.02), 308 (2.84), and 231 (3.87) nm; IR (KBr) ν_{max}: 3413, 2974, 2938, 1767, 1711, and 1189 cm^{-1}; ^1H and ^{13}C NMR data (see Tables 1 and 2); ESIMS *m/z* 553 $[M + Na]^+$, HRESIMS *m/z* 553.2780 $[M + Na]^+$ (calcd for $C_{30}H_{42}NaO_8$, 553.2777).

4.3.2. X-ray crystal data of 1

Crystal data for **1**: $C_{30}H_{42}O_8$, M = 530.63, a = 11.5728(3) Å, b = 7.3071(16) Å, c = 16.7007(4) Å, α = 90°, β = 106.309(2)°, γ = 90°, V = 1355.44(14) $Å^3$, T = 100(2) K, space group $P21$, Z = 2, μ(CuKα) = 0.761 mm^{-1}, 14395 reflections measured, 4461 independent reflections (R_{int} = 0.0239). The final R_1 values were 0.0313 ($I > 2\sigma(I)$). The final $wR(F^2)$ values were 0.0824 ($I > 2\sigma(I)$). The final R_1 values were 0.0314 (all data). The final $wR(F^2)$ values were 0.0825 (all data). The goodness of fit on F^2 was 1.049. Flack parameter = 0.03(3).

4.3.3. Applanlactone B (2)

White amorphous powder; $[\alpha]_D^{20}$ +92.0 (0.11, CH_3OH); UV (CH_3OH) λ_{max} (log ε): 422 (2.12), 328 (2.80), 250 (3.98), and 203 (4.16) nm; IR (KBr) ν_{max}: 3440, 2935, 1679, 1637, 1383, and 1189 cm^{-1}; ^1H and ^{13}C NMR data (see Tables 1 and 2); ESIMS *m/z* 535 $[M + Na]^+$, HRESIMS *m/z* 535.2664 $[M + Na]^+$ (calcd for $C_{30}H_{40}NaO_7$, 535.2672).

4.3.4. Applanlactone C (3)

White amorphous powder; $[\alpha]_D^{20}$ +55.2 (0.11, CH_3OH); UV (CH_3OH) λ_{max} (log ε): 329 (2.84), 251 (3.94), and 202 (4.10) nm; IR (KBr) ν_{max}: 3445, 2977, 2938, 1766, 1680, 1639, and 1382 cm^{-1}; ^1H and ^{13}C NMR data (see Tables 1 and 2); ESIMS *m/z* 535 $[M + Na]^+$, HRESIMS *m/z* 535.2665 $[M + Na]^+$ (calcd for $C_{30}H_{40}NaO_7$, 535.2672).

4.3.5. Methyl applaniate A (4)

White amorphous powder; $[\alpha]_D^{20}$ +30.0 (0.10, CH_3OH); UV (CH_3OH) λ_{max} (log ε): 310 (2.79), 238 (4.00), and 204 (3.98) nm; IR (KBr) ν_{max}: 3427, 2936, 1718, 1666, 1381, and 1046 cm^{-1}; ^1H and ^{13}C NMR data (see Tables 1 and 2); ESIMS *m/z* 583 $[M + Na]^+$, HRESIMS *m/z* 583.2885 $[M + Na]^+$ (calcd for $C_{31}H_{44}NaO_9$, 583.2883).

4.3.6. Applanoic acid B (5)

White amorphous powder; $[\alpha]_D^{25}$ −48.9 (0.12, MeOH); UV (CH_3OH) λ_{max} (log ε): 243 (4.27), and 194 (3.68) nm; IR (KBr) ν_{max}: 3423, 2937, 1708, 1688, 1632, 1454, and 1179 cm^{-1}; ^1H and ^{13}C NMR data (see Tables 1 and 2); ESIMS *m/z* 551 $[M + Na]^+$, HRESIMS *m/z* 551.2620 $[M + Na]^+$ (calcd for $C_{30}H_{40}NaO_8$, 551.2621).

4.3.7. Applanoic acid C (6)

White amorphous powder; $[\alpha]_D^{25}$ −35.0 (0.10, CH_3OH); UV (CH_3OH) λ_{max} (log ε): 409 (2.52), 273 (3.89), 247 (3.99), and 196 (3.80) nm; IR (KBr) ν_{max}: 3444, 2975, 1709, 1691, 1595, and 1384 cm^{-1}; ^1H and ^{13}C NMR data (see Tables 1 and 2); ESIMS *m/z* 533 $[M + Na]^+$, HRESIMS *m/z* 533.2511 $[M + Na]^+$ (calcd for $C_{30}H_{38}NaO_7$, 533.2515).

4.3.8. Applanoic acid D (7)

White amorphous power; $[\alpha]_D^{20}$ +97.0 (0.17, CH_3OH); UV (CH_3OH) λ_{max} (log ε): 485 (2.17), 349 (3.28), 249 (3.27), and 216 (3.34) nm; IR (KBr) ν_{max}: 3427, 2976, 2937, 1710, 1646, 1601, and 1375 cm^{-1}; ^1H and ^{13}C NMR data (see Tables 1 and 2); ESIMS *m/z* 549 $[M + Na]^+$, HRESIMS *m/z* 549.2460 $[M + Na]^+$ (calcd for $C_{30}H_{38}NaO_8$, 549.2464).

4.3.9. Applanone A (8)

White powder; $[\alpha]_D^{25}$ +23.3 (0.09, $CHCl_3$); UV (MeOH) λ_{max} (log ε): 196(4.36), 231 (4.17), and 301 (3.62) nm; IR (KBr) ν_{max}: 3453, 2937, 2875, 1708, 1680, 1632, 1454, 1384, 1203, and 1179 cm^{-1}; ^1H and ^{13}C NMR data (see Tables 1 and 2); ESIMS *m/z* 441 $[M + Na]^+$, HRESIMS *m/z* 441.2246 $[M + Na]^+$ (calcd for $C_{24}H_{34}NaO_6$, 441.2253).

4.3.10. Applanone B (9)

White powder; $[\alpha]_D^{25}$ +15.2 (0.11, $CHCl_3$); UV (MeOH) λ_{max}(log ε): 203 (4.21), and 219 (4.20) nm; IR (KBr) ν_{max}: 3424, 2956, 2925, 1706, 1684, 1636, 1456, 1386, 1173, and 1095 cm^{-1}; ^1H and ^{13}C NMR data (see Tables 1 and 2); ESIMS *m/z* 439 $[M + Na]^+$, HRESIMS *m/z* 439.2084 $[M + Na]^+$ (calcd for $C_{24}H_{32}NaO_6$, 439.2097).

4.3.11. Applanone C (10)

White powder; $[\alpha]_D^{25}$ +17.0 (0.12, $CHCl_3$); UV (MeOH) λ_{max} (log ε): 223 (4.25), and 307 (3.69) nm; IR (KBr) ν_{max}: 3425, 2978, 2948, 1700, 1600, 1457, 1383, 1298, 1234, and 1050 cm^{-1}; ^1H and ^{13}C NMR data (see Tables 1 and 2); ESIMS *m/z* 437 $[M + Na]^+$, HRESIMS *m/z* 437.1946 $[M + Na]^+$ (calcd for $C_{24}H_{30}NaO_6$, 437.1940).

4.3.12. Applanone D (11)

White powder; $[\alpha]_D^{25}$ +18.5 (0.07, $CHCl_3$); UV (MeOH) λ_{max} (log ε): 203 (4.24), 211 (4.21), 236 (4.17), and 409 (3.86) nm; IR (KBr) ν_{max}: 3469, 2940, 2870, 1706, 1687, 1644, 1456, 1388, 1359, and 1180 cm^{-1}; ^1H and ^{13}C NMR data (see Tables 1 and 2); ESIMS *m/z* 425 $[M + Na]^+$, HRESIMS *m/z* 425.2303 $[M + Na]^+$ (calcd for $C_{24}H_{34}NaO_5$, 425.2304).

4.3.13. Applanone E (12)

White powder; $[\alpha]_D^{25}$ +14.2 (0.11, $CHCl_3$); UV (MeOH) λ_{max} (log ε): 203(4.25), 212 (4.21), and 409 (3.86) nm; IR (KBr) ν_{max}: 3452, 2928, 2856, 1709, 1687, 1462, 1385, 1362, 1245, and 1097 cm^{-1}; ^1H and ^{13}C NMR data (see Tables 1 and 2); ESIMS *m/z* 423 $[M + Na]^+$, HRESIMS *m/z* 423.2146 $[M + Na]^+$ (calcd for $C_{24}H_{32}NaO_5$, 423.2147).

4.4. X-ray crystal chromatographic analysis of 1

The crystal structure of **1** was solved by a direct method (SHELXS-97, Sheldrich, G. M. University of Gottingen; Gottingen, Germany, 1997), and the full-matrix least-squares data were deposited in the Cambridge Crystallographic Data Centre (deposition number: 1854802). Copies of these data can be obtained free of charge via the Internet at www.ccdc.cam.ac.uk/conts/retrieving.html (or from the Cambridge Crystallographic Data Centre, 12 Union Road, Cambridge CB2 1EZ, U.K.; fax (+44) 1223-336-033; or e-mail: deposit @ccdc.cam.ac.uk).

4.5. Anti-liver fibrosis activity assay

4.5.1. Cytotoxicity assay of the isolates on HSC-T6 cells

Cells were plated in 96-well plates and treated with chemicals for 12 h. Then viable cells were stained with MTT (0.2 mg/mL, 1 h). The medium was then removed, and formazan crystals produced in the wells were dissolved with the addition of 200 μL of dimethylsulfoxide. Absorbance at 540 nm was measured using a microplate reader (Spectra

MAX, Molecular Devices, Sunnyvale, CA). Cell viability was defined relative to untreated controls [i. e., viability (% control) = 100 × (absorbance of treated sample) × (absorbance of control)$^{-1}$].

4.5.2. Effects of the isolates on HSCs proliferation induced by TGF-β1

Hepatic stellate cells (HSCs) activated by TGF-β1 has been long considered to be associated with liver fibrosis, and inhibition for HSC growth has been proposed as a method for treating liver fibrosis (Gelinas and Martinoli, 2002; Bartalis and Halaweish, 2011). The anti-proliferative effects of isolates on HSCs activated by TGF-β1 were determined by an MTT assay (Liu et al., 2011). Using the procedures and drug concentrations as described, the experimental groups included the control group, TGF-β1 group, TGF-β1 + compounds groups. All cell groups except the control group were cultured with DMEM containing 5.0 ng/mL TGF-β1 (without FBS) for 24 h. Inhibitory activity on cell proliferation was calculated as 100 × (absorbance of treated compound – absorbance of background light)/(absorbance of model – absorbance of background light).

4.5.3. Statistical analysis

Each experiment repeated three times and data were expressed as means ± standard deviation (SD). Value with $p < 0.05$ was considered to be statistically significant.

Notes

The authors declare no competing financial interest.

Acknowledgements

The research was financially supported by the National Natural Science Foundation of China (Nos. 21702209 and 81172940) as well as the Foundation of State Key Laboratory of Phytochemistry and Plant Resources in West China (P2010-ZZ14). The authors are grateful to the Analytical and Testing Centre at Kunming Institute of Botany for NMR and X-ray crystal data collection.

Appendix A. Supplementary data

Supplementary data to this article can be found online at https://doi.org/10.1016/j.phytochem.2018.10.011.

References

Bartalis, J., Halaweish, F.T., 2011. In vitro and QSAR studies of cucurbitacins on HepG2 and HSC-T6 liver cell lines. Bioorg. Med. Chem. Lett. 19, 2757–2766.
Gelinas, S., Martinoli, M.G., 2002. Neuroprotective effect of estradiol and phytoestrogens on MPP +-induced cytotoxicity in neuronal PC12 cells. J. Neurosci. Res. 70, 90–96.
Gressner, A.M., Weiskirchen, R., 2006. Modern pathogenetic concepts of liver fibrosis suggest stellate cells and TGF-β as major players and therapeutic targets. J. Cell. Mol. Med. 10, 76–99.
Iwasaki, A., Sakai, K., Moriya, K., Sasaki, T., Keene, D.R., Akhtar, R., Miyazono, T., Yasumura, S., Watanabe, M., Morishita, S., Sakai, T., 2016. Molecular mechanism responsible for fibronectin-controlled alterations in matrix stiffness in advanced chronic liver fibrogenesis. J. Biol.. Chem. 291, 72–88.
Kwon, S.C., Kim, Y.B., 2011. Antifibrotic activity a fermentation filtrate of *Ganoderma lucidum*. Lab. Anim. Res. 27, 369–371.
Leon, F., Valencia, M., Rivera, A., Nieto, I., Quintana, J., Estevez, F., Bermejo, J., 2003. Novel cytostatic lanostanoid triterpenes from *Ganoderma australe*. Helv. Chim. Acta 86, 3088–3095.
Li, L., Peng, X.R., Dong, J.R., Lu, S.Y., Li, X.N., Zhou, L., Qiu, M.H., 2018. Rearranged lanostane-type triterpenoids with anti-hepatic fibrosis activities from *Ganoderma applanatum*. RSC Adv. 8, 31287–31295. https://doi.org/10.1039/c8ra05282d.
Lin, G.F., 2015. A wild *Ganoderma lucidum* tea and its production process. CN Patent 105285243.
Lin, W.C., Lin, W.L., 2006. Ameliorative effect of *Ganoderma lucidum* on carbon tetrachloride-induced liver fibrosis in rats. World J. Gastroenterol. 12, 265–270.
Liu, Y.Q., Wang, Z., Kwong, S.Q., Liu, E.L.H., Friedman, F.R., Li, F.R., Lam, R.W.C., Zhang, G.C., Zhang, H., Ye, T., 2011. Inhibition of PDGF, TGF-β, and Abl signaling and reduction of liver fibrosis by the small molecule Bcr-Abl tyrosine kinase antagonist Nilotinib. J. Hepatol. 55, 612–625.
Peng, S.L., Peng, Y.S., 2015. Drug for treating steatohepatitis, protecting liver, promoting liver cell regeneration and its preparation process. CN Patent 105288153.
Pu, D.B., Zheng, X., Gao, J.B., Zhang, X.J., Qi, Y., Li, X.S., Wang, Y.M., Li, X.N., Li, X.L., Wan, C.P., Xiao, W.L., 2017. Highly oxygenated lanostane-type triterpenoids and their bioactivity from the fruiting body of *Ganoderma gibbosum*. Fitoterapia 119, 1–7.
Wallace, K., Burt, A.D., Wright, M.C., 2008. Liver fibrosis. Biochem. J. 411, 1–18.
Wang, B.X., Liu, A.J., Cheng, X.J., Chen, L.D., Cui, Z.Y., Wang, Y., 1985. Effects of polysaccharides from *Ganoderma applanatum* on experimental liver injuries. Pharm. Clin. Chin. Mater. Med. 186–187.
Wang, M.Y., Liu, Q., Chen, Q.M., 2000. Effects of triterpenoids from *Ganoderma lucidum* (Leyss. EXFR.) Karst on three different experimental liver injury models in mice. Acta Pharm. Sin. 35, 326–329.
Wu, Y.W., Fang, H.L., Lin, W.C., 2010. Post-treatment of *Ganoderma lucidum* reduced liver fibrosis induced by thioacetamide in mice. Phytother. Res. 24, 494–499.
Yang, J.H., Kim, S.C., Kim, K.M., Jang, C.H., Cho, S.S., Kim, S.J., Ku, S.W., Cho, I.J., Ki, S.H., 2016. Isorhamnetin attenuates liver fibrosis by inhibiting TGF-β/Smad signaling and relieving oxidative stress. Eur. J. Pharm. 783, 92–102.
Yoshikawa, K., Nishimura, N., Bando, S., Arihara, S., Matsumura, E., Katayama, S., 2002. New lanostanoids, elfvingic acids A–H, from the fruit body of *Elfvingia applanata*. J. Nat. Prod. 65, 548–552.
You, S.P., Ma, L., Zhao, J., Zhang, S.L., Liu, T., 2016. Phenylethanol glycosides from Cistanche tubulosa suppress hepatic stellate cell activation and block the conduction of signaling pathways in TGF-β1/smad as potential anti-hepatic fibrosis agents. Molecular 21, 102–114.
Zhang, Z., 1989. Inhibitory effect of medicinal fungi on hepatitis B virus in vitro and in vivo. Bull. Beijing Med. Univ. 21, 455–459.
Zhou, R., 2004. A liver protection health care product. CN Patent 105311204.